

Mineral chemistry and petrogenesis of carbonatite intrusions, Perry and Conway Counties, Arkansas

GEORGE R. McCORMICK, RICHARD C. HEATHCOTE*

Department of Geology, University of Iowa, Iowa City, Iowa 52242, U.S.A.

ABSTRACT

Xenocrystic alvikite (C_2) breccia containing fragmental xenoliths of magnetite-apatite rock, phlogopite, and argillite together with xenoliths of granite, syenite, and two varieties of sovite (C_1) all exhibiting reaction rims are described from Morrilton, Oppelo dump, Perryville, and Brazil Branch, Arkansas. The texture indicates that the bodies were explosively emplaced, and anorthoclase and aegirine in syenite xenoliths indicate that fenitization preceded one or more of the carbonatite intrusive phases.

The mica chemistry indicates that green phlogopite represents remnants of the earliest (C_1) sovite intrusive phase, and golden yellow, reversed pleochroic, phlogopite represents the metasomatized or "dolomitized" phase of the C_1 sovite. The metasomatism introduced Si, Mg, and Fe^{3+} and removed Fe^{2+} , Al, and Ti from the magma.

Zoned pyroxene and amphibole phenocrysts and xenocrysts from the C_1 sovite indicate that the C_1 magma was being enriched in Mg and losing Fe; there is also a slight increase in Ti and Al. All ferromagnesian xenocrysts show magnetite-bearing reaction rims where they are in contact with the C_2 alvikite, which suggests oxidation of the alvikite magma.

Eastonite, which is present as overgrowths around reaction rims on a number of phlogopite xenocrysts, contains Ba and also the highest percentage of Al and Mg of all the micas. This eastonite may represent a C_4 alvikite phase, but in any case crystallized after the formation of the Fe-Ti reaction rim.

INTRODUCTION

Four of six small carbonatite breccia pipes and sills in the vicinity of Oppelo and Perryville in Conway and Perry Counties in west-central Arkansas are still exposed. They trend in a north-south line from Morrilton to Brazil Branch (Fig. 1). Four sills at one locality, known as the Arkansas River sills, were first recognized in 1888 (Williams, 1890), but not studied until 1927 during the mapping of the Arkoma basin. Croneis found additional breccia pipes at Oppelo, Perryville, and Brazil Branch (now Tyndal Slough) and described them as lamprophyres whose groundmass had been altered to secondary calcite (Croneis and Billings, 1930). Steele and Wagner (1979) described sills from Morrilton Dam and from a shale pit on Highway 113, called the Oppelo dump locality. A natural gas well drilled west of Oppelo in sec. 8, T5N, R17W passed through 41 carbonatites, some as much as 30 ft (9.1 m) thick, to a total depth of 11 850 ft (3612 m) (Mitchell, 1979).

Steele and Wagner (1979) published several analyses of the carbonatite matrix of the various intrusions but not of the xenoliths. Mitchell (1979) described the igneous xenoliths in the Oppelo dump and Brazil Branch bodies and speculated on their origin and geologic history.

The breccia pipes are composed of alvikite containing

silicate xenoliths, sovite xenoliths, and xenocrysts of ferromagnesian minerals, magnetite, and apatite; overgrowths on phlogopite xenocrysts may represent a more evolved carbonatite phase. The present mineralogical study has been undertaken to document the chemical changes that occurred during successive phases of carbonatite emplacement.

GEOLOGIC SETTING

The carbonatite bodies in this study are the northernmost known in the Arkansas igneous province. They lie on the north side of the Ouachita fold belt, 47 to 71 km north of the Magnet Cove alkaline carbonatite complex that crops out in the interior of the Ouachita structural province (Fig. 2). The frontal Ouachita Mountains comprise an east-trending structural belt characterized by thrust faults and steep, narrow folds that are locally overturned. The Arkoma basin, a contiguous structural province north of the Ouachita belt, contains less faulting and broad, low-amplitude folds. The country rock in the vicinity of the carbonatite bodies is a siliciclastic sequence of the Ouachita flysch facies of Atokan Age.

Southwest of the Brazil Branch locality, high-altitude photography shows a tear fault trending N15–20°E and cutting across the Ouachita structural grain; this fault is on strike with the Brazil Branch, Perryville, and Morrilton carbonatite outcrops; the Oppelo dump exposure is only slightly to the east of this line. The alignment of the carbonatite breccias and sills parallel with regional lineaments of the Ouachita Mountains and northern Arkansas suggests that their emplacement was controlled by

* Present address: Core Laboratories, Inc., 10703 E. Bethany Drive, Aurora, Colorado 80014, U.S.A.

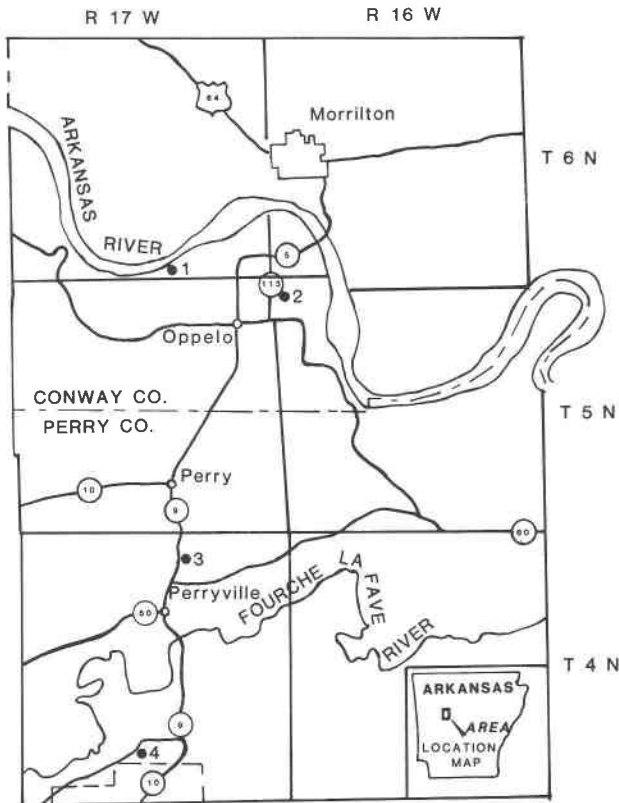


Fig. 1. Location map of study area and carbonatite intrusions: (1) Morrilton Dam, (2) Oppelo dump, (3) Perryville, (4) Brazil Branch.

basement faulting, as is common in many carbonatite provinces (Heinrich, 1980).

METHOD OF INVESTIGATION

Approximately 500 analyses were obtained on the ARL-EMX-SM electron microprobes at the University of Chicago and the University of Iowa using the following standards: Asbestos microcline (K); Amelia albite (Na, Al, Si); $Di_{85}Jd_{15}$ glass (Mg); An_{50} glass (Ca); A-128 ilmenite (Ti); hortonolite (Mn, Fe); and P-140 olivine (Si, Mg, Fe). Kakanui hornblende was used as a working standard for all these elements. Analytic conditions were spot size 4 to 18 μ m, counting time 60 s, accelerating voltage 15 kV with 1000 nA, and detection level for all elements approximately 0.2 wt% (1σ). Background and peak counts were determined by the procedures of Reed and Ware (1975); corrections were made with Bence-Albee factors (1968).

Selected representative analyses are presented in Tables 1-4; all analyses were used as the data base for Figures 3-7. Additionally, reconnaissance analyses with the wavelength-dispersive method disclosed no discernible differences among several generations of apatite in La, Ce, Sr, Y, Cl, or F amounts. Ti values for phlogopite rims obtained by EDS (Table 2) are considered suspect because reconnaissance WDS analyses of a few Perryville samples indicate that Ba (whose EDS peak overlaps that of Ti) is always present in eastonitic overgrowths in amounts greater than 1 wt%.

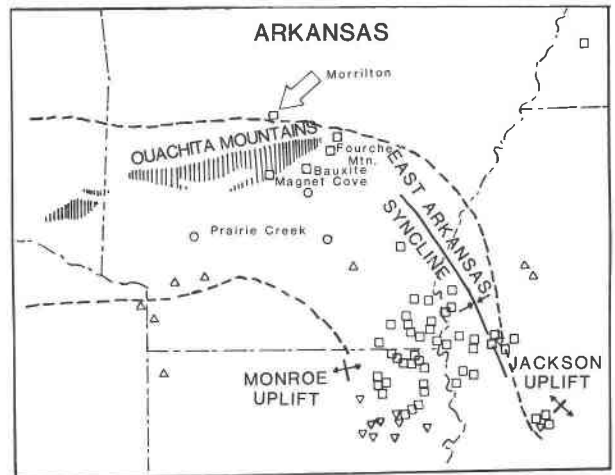


Fig. 2. The Arkansas alkalic province. Study area shown by arrow; map modified from Erickson and Blade (1963). \square = Cretaceous alkalic intrusive and volcanic rocks; ∇ = Cretaceous basic volcanic rocks; \circ = Cretaceous ultrabasic intrusive rocks; \triangle = pre-Cretaceous diabase and basalt. Vertical-line pattern indicates structurally and topographically high areas; axes of anticlines and synclines are shown by appropriate arrows.

MEGASCOPIC TEXTURES

Carbonatite samples from all four localities are light gray when freshly broken and reddish brown when weathered. All are xenocrystic alvikite breccias that contain xenoliths of granite, syenite, magnetite-apatite rock, sovite, phlogopite, and argillite. The granite, syenite, and sovite xenoliths range in size from less than 2 mm up to 5 cm, are well rounded, and exhibit reaction rims with the groundmass. The sovite xenoliths are armored by medium to finely crystalline calcite. Magnetite-apatite rock and phlogopite xenoliths are fragmental and generally less than 1 cm in diameter. The argillite xenoliths are generally wedge shaped and from less than 2 mm up to 9 cm, with an average length of 2-3 cm. Pale reaction rims on the black argillite xenoliths are visible megascopically in the Brazil Branch and Morrilton Dam samples; this type of xenolith was not found in the Perryville or Oppelo dump samples.

The abundance of xenoliths is far greater in the Brazil Branch and Morrilton samples than in the Perryville or Oppelo dump samples. The majority of xenoliths in the Brazil Branch samples are argillite, and those from Morrilton Dam are syenites and granites. Phlogopite xenoliths are found only in the Morrilton Dam samples. Magnetite-apatite rock xenoliths and sovite xenoliths are found at all four localities.

Xenocrysts of phlogopite, clinopyroxene, amphibole, apatite, and magnetite are common in all samples. Xenocryst maximum sizes are phlogopite, 10 mm; clinopyroxene, 8 mm; amphibole, 6 mm; and magnetite and apatite, 10 mm. Phlogopite is more common than clinopyroxene and amphibole; amphibole is less abundant than clino-

Table 1. Chemical composition of magnetite (EDS microprobe data)

	P1-6-A SX	P1-X-11 SX	P1-10-C R	M15-9-M MA	M18-6-A SX	M18-3-C R	M4-5-H R	OD6-16-13 SX	OD6-5-A R
MgO	2.71	2.75	4.11	2.77	2.87	2.39	2.74	3.14	3.48
Al ₂ O ₃	0.53	0.48	4.40	0.89	0.62	0.72	0.77	0.96	3.87
SiO ₂	0.26	0.26	0	0	0.16	0	0.16	0	0.38
CaO	0.24	0.43	0.29	0.22	0.13	0	0	0	0.18
TiO ₂	8.00	8.17	11.74	10.34	8.85	10.83	10.63	9.44	13.88
MnO	1.21	0.94	0.52	1.07	1.19	1.06	0.95	1.01	0.39
FeO	81.86	82.59	75.26	79.33	80.97	78.37	78.72	81.94	77.12
V ₂ O ₅	—	—	—	0.39	0.36	0.37	0.33	—	—
Sum	94.82	95.62	96.32	95.03	95.13	93.72	94.29	96.49	99.29
Numbers of ions on the basis of 24 atoms of oxygen									
Mg	1.11	1.12	1.55	1.11	1.16	0.97	1.11	1.25	1.26
Al	0.17	0.15	1.31	0.28	0.20	0.23	0.24	0.30	1.11
Si	0.07	0.07	0	0	0.04	0	0.04	0	0.09
Ca	0.07	0.12	0.08	0.07	0.04	0	0	0	0.05
Ti	1.65	1.67	2.23	2.09	1.81	2.22	2.16	1.89	2.54
Mn	0.28	0.22	0.11	0.25	0.27	0.25	0.22	0.23	0.08
Fe	18.83	18.82	15.86	17.84	18.41	17.88	17.80	18.28	15.69
V	—	—	—	0.01	0.08	0.08	0.07	—	—

Note: Locations are shown by the letters in the sample numbers: M = Morrilton, OD = Oppelo dump, P = Perryville. Other abbreviations: SX = sovite xenolith, R = reaction rim, MA = magnetite-apatite xenolith.

pyroxene in all but the Brazil Branch samples (in which it is subequal).

COMPOSITION OF THE GROUNDMASS

The groundmass of all but the Brazil Branch samples is a finely crystalline mosaic of calcite, apatite, and an unidentified green, highly birefringent mineral (possibly a ferromagnesian mineral that has altered to clay). Moderate amounts of magnetite, phlogopite, dolomite, and accessory perovskite, zircon, and pyrite are also usually present. The phlogopite of the groundmass is eastonitic, similar in composition to overgrowths found on phlogopite xenocrysts. The Morrilton Dam alvikite contains thin veins (<2 mm thick) of calcite and vugs of ferroan calcite and dolomite.

The texture of the groundmass in the Brazil Branch samples features rhomboid to tabular crystals of calcite in a microcrystalline apatite-bearing matrix. The groundmass of the Brazil Branch alvikite differs in having an abundance of acicular aegirine crystals grown together in clots adjacent to agillite xenoliths.

MINERAL CHEMISTRY OF XENOCRYSTS

Textural evidence such as fragmental shapes, corroded edges, and reaction rims on the ferromagnesian minerals in all of the alvikites indicate that these minerals (phlogopite, clinopyroxene, and amphibole) are xenocrysts. The larger magnetite and apatite grains are also considered to be xenocrysts, a deduction based on the similarity of composition (Table 1) and intergrowth textures to the magnetite-apatite rock xenoliths. A separate generation of magnetite grains—which contain no apatite inclusions and are commonly attached to ferromagnesian grains or are present as isolated grains in the groundmass—formed as a reaction product between the ferromagnesian xenocrysts and the alvikitic liquid.

Phlogopite. Two types of phlogopite xenocrysts are present: (1) a pale golden-yellow variety with weakly reverse to normal pleochroism and (2) a green to colorless or pale green strongly normal pleochroic variety. The green phlogopite contains more Al in the tetrahedral site, a wider range of Fe/(Fe + Mg) in the octahedral site, and higher Ti content than the golden-yellow variety (Figs. 3, 4). Green phlogopites are occasionally zoned, the outer zone being more Fe rich; golden-yellow phlogopites are rarely zoned with no discernible compositional gradients. Golden-yellow phlogopite contains insufficient Al and Si to fill tetrahedral sites, and we suspect that Fe³⁺ fills the site.

Edges of xenocrystic phlogopite in all samples exhibit rounding and formation of magnetite-bearing reaction rims. Xenocrysts often have overgrowths around the reaction rims of very pale greenish-white eastonitic mica containing more Al and Mg (Table 2; Figs. 3, 4). Reconnaissance wds analyses of these overgrowths indicate Ba in amounts estimated to be as high as 5 wt%, and TiO₂ generally in trace amounts only. All analyses of green rims (Table 2) exhibit low totals that may also reflect the problem with Ti vs. Ba in the analyses.

Clinopyroxene. Xenocrystic clinopyroxene is euhedral to idiomorphic fragmental with scalloped and embayed margins. It is weakly zoned and has microcrystalline reaction rims containing magnetite. The compositions of clinopyroxene xenocrysts from all four localities are salitic and nearly identical. Xenocrysts from Brazil Branch, however, exhibit a greater variation in Na and Fe content than those from other localities (Table 3, Fig. 5). Analyses for Mg, Fe, and Ca (Fig. 6) of cores of clinopyroxene xenocrysts exhibit moderate scatter, whereas analyses of rims are clustered. The rims are all slightly more calcic.

Amphibole. Amphibole xenocrysts have scalloped and embayed margins indicating reaction with the groundmass; the outer zones (clearly overgrowths on some grains)

Table 2. Chemical composition of phlogopite and biotite (EDS microprobe data)

	BB1- 18-2 GC	BB1- 18-1 GR	BB1- 4-1 YC	BB2- 16-2 GP	OD6- 3-1 GC	OD6- 3-2 GR	OD1- 13-1 GC	OD1- 13-2 GR	P2- 3-1 YC	P2- 3-2 YR	P1- 11-2 YC	P1- 4-6 GC	P1- 4-7 GR	
SiO ₂	35.73	35.90	37.65	37.53	37.02	34.12	39.28	34.08	42.01	32.55	40.69	37.66	33.86	
TiO ₂	3.81	3.33	2.61	2.15	3.78	2.15	2.15	2.86	0.72	3.70	1.12	4.60	3.13	
Al ₂ O ₃	17.11	17.86	12.10	13.57	15.80	20.61	13.70	20.44	11.30	21.90	11.86	16.76	21.70	
FeO	13.25	12.37	22.74	17.17	13.92	4.88	10.72	5.63	8.74	5.98	9.16	9.36	5.48	
MnO	0	0	0.39	0.30	0	0.33	0	0.27	0	0	0	0	0.38	
MgO	3.70	16.97	11.97	14.86	16.56	21.75	20.54	21.27	22.95	20.41	22.75	19.18	21.46	
CaO	0.37	0.22	0.32	0.31	0	0.40	0.39	0.53	0.63	0.47	0.53	0.37	0.47	
Na ₂ O	0.40	0	0.41	0.39	0	0	0.44	0	0.44	0	0	0.55	0	
K ₂ O	9.36	9.39	8.86	8.93	9.54	8.92	9.33	8.59	7.59	7.9	9.20	9.50	8.85	
Sum	96.99	96.04	97.05	95.22	96.63	93.17	96.56	93.67	94.39	92.91	95.31	97.99	95.33	
Numbers of ions on the basis of 22 atoms of oxygen														
Si	5.22	5.25	5.74	5.68	5.43	4.98	5.67	4.96	6.06	4.76	5.89	5.34	4.84	
Ti	0.42	0.37	0.30	0.24	0.42	0.24	0.23	0.31	0.08	0.41	0.12	0.49	0.34	
Al(IV)	2.78	2.95	2.18	2.32	2.57	3.02	2.33	3.04	1.92	3.24	2.02	2.66	3.16	
Al(VI)	0.17	0.33	0	0.10	0.16	0.52	0.01	0.46	0	0.54	0	0.14	0.50	
Fe(IV)	0	0	0.08	0	0	0	0	0	0.02	0	0.09	0	0	
Fe(VI)	1.62	1.52	2.82	2.17	1.71	0.60	1.29	0.69	1.04	0.73	1.02	1.11	0.66	
Mn	0	0	0.05	0.04	0	0.04	0	0.03	0	0	0	0	0.05	
Mg	3.70	3.70	2.72	3.35	3.62	4.73	4.42	4.61	4.93	4.45	4.91	4.05	4.57	
Ca	0.06	0.03	0.05	0.05	0	0.06	0.06	0.08	0.10	0.07	0.08	0.06	0.07	
Na	0.11	0	0.12	0.12	0	0.12	0.12	0	0.12	0	0	0.15	0	
K	1.74	1.75	1.72	1.72	1.78	1.72	1.72	1.59	1.40	1.48	1.70	1.71	1.62	
	P2- 17-2 GC	P2- 17-3 GR	P2- 13-1 GC	P2- 13-2 GR	M17- 3-A GC	M30- 7-E GC	M16-1 YC	M16-2 YR	MX- 4-3 GC	MX- 4-1 GR	M18- 4-A YP	M18- 4-B YP	M7- 7-D S	M7- 10-G S
SiO ₂	37.12	32.51	37.25	32.00	37.27	38.06	39.30	31.05	37.10	32.00	40.80	40.59	38.24	38.63
TiO ₂	3.81	3.75	3.97	4.14	3.25	4.74	1.14	3.37	4.18	2.07	1.53	1.47	2.91	2.62
Al ₂ O ₃	16.81	22.75	16.67	22.53	15.58	16.40	10.67	21.37	15.95	19.51	12.56	12.39	13.56	14.13
FeO	14.01	5.85	13.29	5.70	13.40	7.98	7.49	5.68	11.56	4.79	10.03	9.59	16.58	17.00
MnO	0	0.41	0	0.30	0	0	0.24	0.13	0	0.25	0	0	0	0.21
MgO	16.80	21.08	17.44	20.85	16.73	19.29	22.66	20.11	16.99	20.04	21.29	21.52	14.16	13.93
CaO	0.31	0.87	0.27	0.49	0	0	0.31	0.64	0.57	2.46	0	0	0	0
Na ₂ O	0.42	0	0.54	0	0.26	0.53	0.43	0.40	0.61	0.19	0.63	0.50	0.22	0.30
K ₂ O	9.44	8.24	9.40	8.38	9.90	9.92	9.84	8.01	8.62	8.70	9.88	9.84	10.26	10.51
Sum	98.72	95.44	98.83	94.47	96.39	96.92	92.09	90.76	95.58	90.02	96.68	95.84	95.93	97.32
Number of ions on the basis of 22 atoms of oxygen														
Si	5.33	4.65	5.33	4.63	5.48	5.41	5.90	4.68	5.42	4.89	5.86	5.87	5.74	5.73
Ti	0.41	0.40	0.43	0.45	0.36	0.51	0.13	0.38	0.46	0.24	0.17	0.16	0.33	0.29
Al(IV)	2.67	3.35	2.67	3.36	2.52	2.59	1.89	3.32	2.58	3.11	2.13	2.11	2.26	2.27
Al(VI)	0.18	0.49	0.14	0.48	0.18	0.16	0	0.48	0.17	0.40	0	0	0.14	0.20
Fe(IV)	0	0	0	0	0	0	0.22	0	0	0	0.01	0.02	0	0
Fe(VI)	1.68	0.70	1.59	0.69	1.65	0.95	0.72	0.72	1.41	0.61	1.20	1.14	2.08	2.11
Mn	0	0.05	0	0.50	0	0	0.03	0.02	0	0.03	0	0	0	0.03
Mg	3.60	4.50	3.72	4.50	3.67	4.09	5.07	4.52	3.70	4.56	4.55	4.64	3.17	3.08
Ca	0.05	0.13	0.04	0.08	0	0	0.05	0.10	0.09	0.40	0	0	0	0
Na	0.12	0	0.15	0	0.08	0.53	0.13	0.12	0.17	0.05	0.18	0.14	0.06	0.09
K	1.73	1.50	1.71	1.55	1.86	1.80	1.88	1.54	1.61	1.70	1.81	1.82	1.97	1.99

Note: Locations are shown by the letters in the sample numbers: BB = Brazil Branch, M = Morrilton, OD = Oppelo dump, P = Perryville. Other abbreviations: GC = core of green phlogopite xenocryst, GR = rim of green phlogopite xenocryst, GP = phenocryst of green phlogopite in soelite xenolith, S = silicate xenolith, YC = core of yellow phlogopite xenocryst, YR = rim of yellow phlogopite xenocryst, YP = phenocryst of yellow phlogopite in soelite xenolith; (---) connects core and rim of same grain.

have ferroan pargasite compositions that are similar among all xenocrysts, whereas the cores of the xenocrysts range in composition from ferroan pargasitic hornblende to ferroan pargasite (Table 4, Fig. 7). Some xenocrysts are intergrowths of amphibole and clinopyroxene.

Magnetite and apatite. Magnetite and apatite are present in two distinct size ranges: 0.5–1 mm and less than 0.2 mm. Magnetite grains commonly contain inclusions of carbonate groundmass and apatite (Table 1). Most of the larger magnetite grains are embayed and rounded, indicating reaction with the groundmass. Apatite grains

display unreacted margins; the larger grains are fragmental, the smaller ones euhedral.

MINERAL CHEMISTRY OF SOVITE XENOLITHS

Sovite xenoliths contain abundant phenocrysts of golden-yellow phlogopite and a few pale green clinopyroxene phenocrysts in a groundmass of very coarse-grained calcite, apatite, and magnetite. One xenolith from Brazil Branch contained a green pleochroic phlogopite phenocryst similar in composition to the green phlogopite xenocrysts. Xenoliths always display armored margins of

Table 3. Chemical composition of clinopyroxene (EDS microprobe data)

	BB1-1-1		BB1-1-2		BB2-3-1		BB2-3-2		BB2-3-3		OD1-13-3		OD1-13-4		OD1-16-1			
	C	R	C	C	C	M	R	C	R	C	R	C	R	C	R			
SiO ₂	51.40	50.03	49.92	44.79	44.12	48.13	55.14	44.25	52.95									
TiO ₂	0.29	0.64	0.43	1.90	2.66	1.32	0	2.49	0									
Al ₂ O ₃	2.51	2.63	3.06	7.64	7.94	4.48	0	8.39	0.48									
FeO	14.59	7.91	11.12	9.56	11.47	8.44	4.14	8.84	5.71									
MnO	0.41	0	0	0	0	0	0	0	0									
MgO	8.79	13.44	10.87	10.40	9.55	12.02	16.12	11.19	15.15									
CaO	17.65	23.85	20.87	22.41	21.91	22.92	24.13	23.49	23.80									
Na ₂ O	3.52	0.41	1.40	0.71	1.01	0.61	0.44	0	0.34									
Sum	99.18	98.92	97.66	97.40	98.67	97.93	99.98	98.65	98.42									
Numbers of ions on the basis of 6 atoms of oxygen																		
Si	1.98	1.90	1.93	1.74	1.71	1.85	2.07	1.68	1.99									
Ti	0.01	0.01	0.01	0.06	0.08	0.04	0	0.07	0									
Al(IV)	0.02	0.09	0.07	0.26	0.29	0.15	0	0.32	0.01									
Al(VI)	0.10	0.03	0.07	0.09	0.04	0.05	0	0.06	0.01									
Fe	0.47	0.25	0.36	0.31	0.37	0.27	0.13	0.28	0.18									
Mn	0.01	0	0	0	0	0	0	0	0									
Mg	0.51	0.76	0.63	0.60	0.55	0.69	0.88	0.63	0.85									
Ca	0.73	0.97	0.87	0.94	0.91	0.94	0.95	0.96	0.96									
Na	0.26	0.03	0.11	0.05	0.08	0.05	0.03	0	0.03									
Numbers of ions on the basis of 6 atoms of oxygen																		
	OD1-16-3		M4-3-B		M18-3-A		P1-12-1		P2-22-1		P2-23-1		P2-21-1		M30-5-G		M2-1-A	
	R	C	C	C	C	C	R	R	S	S	S	S	S	S	S	S	S	
SiO ₂	48.24	51.18	54.66	53.78	52.78	50.16	46.58	54.31	54.28									
TiO ₂	1.03	0.66	0	0	0.26	1.14	2.07	1.13	0.90									
Al ₂ O ₃	4.36	2.61	0.38	0.75	1.39	3.48	7.24	1.02	0.82									
FeO	7.49	7.34	5.27	6.23	7.39	8.30	9.69	17.62	20.20									
MnO	0	0	0	0	0	0	0	1.02	0.82									
MgO	13.27	13.09	15.18	15.08	13.74	13.09	11.10	5.84	4.62									
CaO	23.46	23.84	24.83	24.02	23.66	23.71	23.57	11.23	9.61									
Na ₂ O	0	0.71	0.51	0.42	0	0	0.66	8.16	9.19									
Sum	97.85	99.44	100.82	100.28	99.22	99.88	100.93	100.31	100.43									
Numbers of ions on the basis of 6 atoms of oxygen																		
Si	1.85	1.92	2.00	1.98	1.97	1.88	1.75	2.08	2.01									
Ti	0.03	0.02	0	0	0.01	0.03	0.06	0.03	0.02									
Al(IV)	0.16	0.08	0	0.02	0.02	0.12	0.25	0	0									
Al(VI)	0.04	0.04	0.02	0.02	0.04	0.03	0.07	0.05	0.04									
Fe	0.24	0.23	0.16	0.19	0.23	0.27	0.30	0.57	0.63									
Mn	0	0	0	0	0	0	0	0.03	2.03									
Mg	0.76	0.73	0.83	0.83	0.77	0.73	0.62	0.33	0.26									
Ca	0.96	0.96	0.97	0.95	0.95	0.95	0.95	0.46	0.38									
Na	0	0.05	0.04	0.03	0	0	0.05	0.61	0.66									

Note: Locations are shown by the letters in the sample numbers: BB = Brazil Branch, M = Morrilton, OD = Oppelo dump, P = Perryville. Other abbreviations: C = core of xenocryst, M = middle of xenocryst, R = rim of xenocryst, S = silicate xenolith; (---) connects core and rim of same grain.

medium to finely crystalline calcite. A few ferromagnesian phenocrysts in sovite xenoliths protrude into the host groundmass; the protrusion invariably has developed a reaction margin.

Phlogopite. Golden-yellow phlogopites are identical in composition to golden-yellow xenocrysts described previously (Table 2; Figs. 3, 4).

Clinopyroxene. Pale green clinopyroxenes are nonpleochroic to weakly pleochroic and salitic; they have compositions similar to cores of xenocrystic clinopyroxenes (Table 3; Figs. 5, 6).

Magnetite and apatite. Magnetite in sovite xenoliths usually appears as vermiform blebs or regular porous networks often having inclusions of carbonate and euhedral apatite. The composition of sovitic magnetite is similar to that of larger magnetite grains in the alvikite matrix and to xenoliths of magnetite-apatite rock. The magnetite has slightly lower Ti, Mg, Si, and Mn contents than the

magnetite reaction rims on ferromagnesian xenocrysts (Table 1).

MINERAL CHEMISTRY OF SILICATE XENOLITHS

Xenoliths of argillite, granite, and syenite are present in all samples. Representative mineral analyses were obtained for granite and syenite xenoliths. Analyses for mineral grains in the microcrystalline argillite were not obtained.

Granite. Xenoliths of granite are fine grained and equigranular; they contain quartz, K-feldspar [K_{2.56}Na_{0.44}(Al_{3.04}Si_{8.96})O₂₄], zoned plagioclase that varies from core [Na_{1.49}Ca_{1.55}(Al_{4.52}Si_{7.45})O₂₄] to rim [Na_{2.32}Ca_{0.66}(Al_{3.68}Si_{8.32})O₂₄], biotite [K_{1.97}Na_{0.06}(Mg_{3.17}Ti_{0.39}Fe_{2.08}Al_{0.39})(Al_{2.26}Si_{5.74})O₂₀(OH)₄] (Figs 3, 4), and amphibole [(Na_{0.46}K_{0.21}Mg_{0.65}Ti_{0.17}Mn_{0.08}Fe_{1.97}Al_{0.25})(Al_{1.12}Si_{6.88})O₂₀(OH)₂] (Fig. 7).

Syenite. Xenoliths of syenite are fine grained and equigranular; they contain anorthoclase [Na_{1.71}K_{1.19}(Al_{2.99}Si_{9.03})-

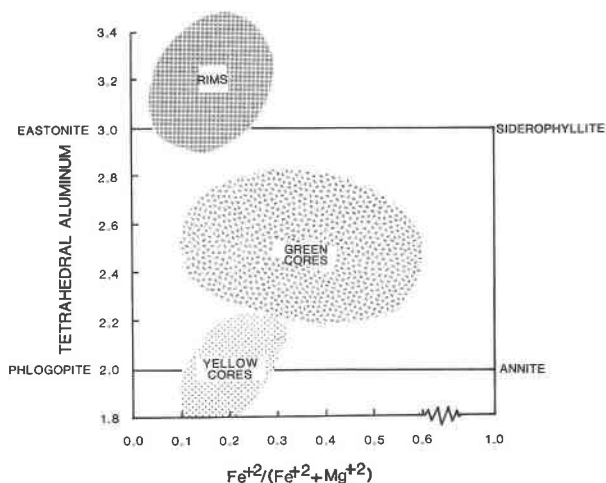


Fig. 3. Compositional varieties of phlogopite-biotite exhibited in terms of atomic percent tetrahedral Al vs. ratio of atomic percent $Fe^{2+}/(Fe^{2+} + Mg^{2+})$. Phlogopite in silicate xenoliths also plots in the "green core" area.

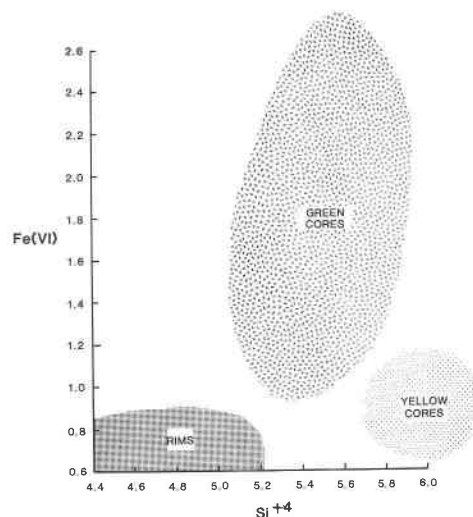


Fig. 4. Compositional varieties of phlogopite exhibited in terms of atomic percent octahedral Fe vs. atomic percent Si^{4+} . Phlogopite in silicate xenoliths also plots in the "green core" area.

O_{24}] and aegirine $[(Na_{2.43}Mg_{1.34}Fe_{2.26}Mn_{0.13}Ti_{0.13}Ca_{1.85}Al_{0.18})-(Si_{8.34})O_{24}]$.

DISCUSSION AND INTERPRETATION

The carbonatite pipes and sills are composed of C_2 alvikite breccia (nomenclature after Le Bas, 1977) containing xenoliths of granite, syenite, argillite, magnetite-apatite rock, phlogopitite, and two varieties of C_1 sovitte together with xenocrysts of ferromagnesian minerals, magnetite, and apatite. Eastonitic overgrowths containing Ba on some phlogopite xenocrysts may represent a late C_4 alvikite phase. The C_3 ferrocarbonatite phase of Le Bas (1977) is not seen.

Textural evidence indicates that these four igneous bodies were explosively emplaced. The source of the magma cannot be determined; however, the presence of xenoliths of granite, syenite, and argillite indicates that the carbonatite originated below or within the crystalline basement. The syenite is composed of anorthoclase and aegirine, which indicate that fenitization preceded one or more of the carbonatite intrusive phases. Angular argillite xenoliths are probably metamorphosed shales of the Ouachita Formation.

The history of carbonatite differentiation and intrusive

Table 4. Chemical composition of amphibole (EDS microprobe data)

	BB1-12-1 C	BB1-12-2 R	BB1-11-1 I	BB1-13-1 C	BB1-13-2 R	OD1-15-5 C	OD1-15-3 R	M11-3-B S	M4-3-L C
SiO ₂	37.61	39.28	39.81	41.62	39.16	39.06	39.94	45.36	39.89
TiO ₂	3.26	2.84	2.36	2.17	2.10	3.36	3.71	1.46	3.10
Al ₂ O ₃	14.42	13.84	11.54	10.59	13.77	14.41	13.98	7.95	13.19
FeO	16.65	12.69	16.67	18.52	12.26	12.55	11.80	15.69	12.15
MnO	0	0	0	0.31	0	0	0	0.55	0
MgO	10.03	12.89	10.62	9.47	13.69	12.39	12.98	11.85	12.56
CaO	11.67	12.25	10.61	9.29	11.86	11.81	11.46	11.54	12.29
Na ₂ O	1.56	1.99	2.66	3.81	1.84	1.57	1.99	1.71	1.76
K ₂ O	2.95	2.78	1.84	1.68	2.36	2.52	2.31	1.13	2.72
Sum	98.14	98.57	95.82	97.46	97.04	97.67	98.16	97.25	97.66
Numbers of ions on the basis of 23 atoms of oxygen									
Si	5.78	5.87	6.15	6.39	5.91	5.86	5.92	6.82	5.99
Ti	0.38	0.32	0.28	0.25	0.24	0.38	0.41	0.17	0.35
Al(IV)	2.22	2.13	1.85	1.61	2.09	2.14	2.08	1.18	2.01
Al(VI)	0.38	0.31	0.26	0.31	0.36	0.40	0.79	0.23	0.32
Fe	2.13	1.59	2.17	2.38	1.55	1.57	1.46	1.97	1.53
Mn	0	0	0	0.04	0	0	0	0.07	0
Mg	2.29	2.87	2.46	2.17	3.08	2.77	2.87	2.66	2.81
Ca	1.91	1.96	1.77	1.53	1.92	1.90	1.82	1.86	1.98
Na	0.46	0.58	0.80	1.14	0.54	0.46	0.57	0.50	0.51
K	0.58	0.53	0.37	0.33	0.45	0.48	0.44	0.22	0.52

Note: Locations are shown by the letters in the sample numbers: BB = Brazil Branch, M = Morrilton, OD = Oppelo dump. Other abbreviations: C = core of xenocryst, R = rim of xenocryst, S = silicate xenolith, I = intergrowth with clinopyroxene; (---) connects core and rim of same grain.

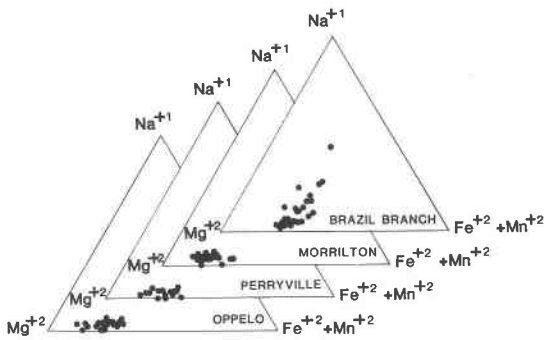


Fig. 5. Variation in clinopyroxene composition exhibited in terms of atomic percent Na^+ , Mg^{+2} , and $\text{Fe}^{+2} + \text{Mn}^{+2}$.

phases is recorded primarily in the chemistry of the micas much as was noted at Oka by Rimsaite (1969). Discontinuous shifts of composition similar to those described by Rimsaite (1969) occur twice in this study: some C_1 green phlogopite was metasomatically altered to C_1 golden-yellow phlogopite and some of both the C_1 green phlogopite and the C_1 golden-yellow phlogopite were altered to eastonite.

Green phlogopite xenocrysts and the single sovite xenolith containing a green phlogopite xenocryst represent remnants of the earliest C_1 sovite intrusive phase. Golden-yellow, reverse pleochroic, unzoned phlogopite is present as phenocrysts in one variety of C_1 sovite xenoliths and as xenocrysts in the C_2 alvikite (Table 2, Fig. 3). This reverse pleochroic phlogopite appears to be similar to the phlogopite that Rimskaya-Korsakova and Sokolova named tetraferriphlogopite (Kapustin, 1980, p. 201). Kapustin described tetraferriphlogopite as an indicator mineral of the "dolomitized" stage of the early carbonatite phase (C_1 of Le Bas, 1977) formed by metasomatic replacement. The dolomitized zones are related to zones of brecciation and schistosity; the brecciation is often associated with linear zones, as is the case here. Analogously, golden-yellow, reverse pleochroic phlogopite xenocrysts and sovite xenoliths containing phenocrysts of reverse pleochroic phlogopite may represent remnants of a metasomatized (dolomitized?) phase of the early C_1 sovite (Ta-

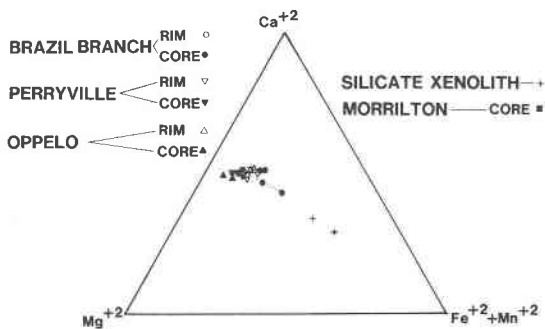


Fig. 6. Variation in clinopyroxene composition exhibited in terms of atomic percent Ca^{+2} , Mg^{+2} , and $\text{Fe}^{+2} + \text{Mn}^{+2}$. Tie lines connect core and rim values of the same grain.

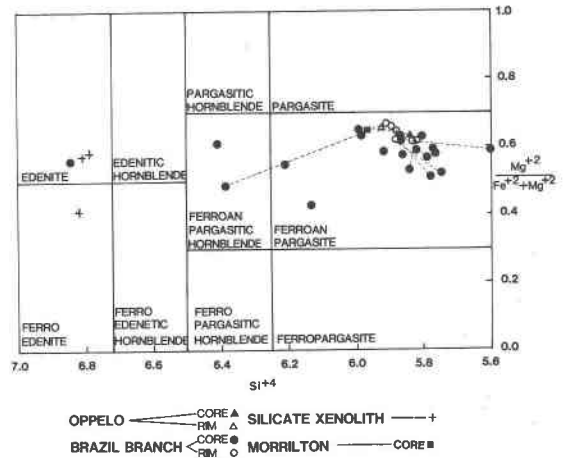


Fig. 7. Variation in amphibole composition exhibited in terms of atomic percent Si^{+4} vs. ratio of atomic percent $\text{Mg}^{+2} / (\text{Mg}^{+2} + \text{Fe}^{+2})$. Tie lines connect core and rim values of the same grain. Modified from Leake (1978).

ble 2; Figs. 3, 4). The phlogopite chemistry (Table 2; Figs. 3, 4) indicates that if the sovite xenoliths that contain golden-yellow phlogopite were formed by metasomatism of the earlier C_1 sovite, Si, Mg, and Fe^{3+} were introduced and Al, Fe^{2+} , and Ti were removed.

Pyroxene and amphibole xenoliths and xenocrysts are weakly zoned. The analyses of the cores indicate slight compositional scatter, whereas the analyses of the rims are clustered (Tables 3, 4; Figs. 6, 7). It appears as though these xenocrysts and phenocrysts formed during the crystallization of the C_1 magma, and therefore the zoning represents changes in chemical composition of the magma during this phase. The compositions of pyroxenes in the C_1 sovite in the Oppelo dump, Perryville, and Morrilton breccias are identical and exhibit little scatter, whereas pyroxene in the Brazil Branch breccia contains more Fe and Na and exhibits greater scatter (Fig. 5). Aegirine is present in the C_2 alvikite phase only in the Brazil Branch specimens, suggesting that the carbonatitic magma at the southern end of this district was more alkaline. Chemical changes from ferromagnesian mineral cores to their rims indicate that the magma was being enriched in Mg and losing Fe; there also is a very slight increase in Ti and Al. This effect could be caused by the precipitation of magnetite or Fe-rich carbonate, which depleted the magma in Fe.

All ferromagnesian mineral xenocrysts in the C_2 alvikite have reaction rims containing magnetite together with many unidentifiable small mineral grains. Magnetites that form in these reaction rims contain higher amounts of Ti, Si, Mg, and Al than xenocrystic magnetites. Such reaction rims suggest oxidation of the alvikite magma in a silica-poor analogue to the oxidation of annite described by Wones and Eugster (1959).

Eastonitic overgrowths that contain more Mg and Al than the other phlogopites are present on the groundmass side of reaction rims on a number of phlogopite xeno-

crysts. wds analysis has shown that these rims contain Ba much as that reported by Gaspar and Wyllie (1982) in phlogopites from Jacupiranga. This eastonite, which may represent a C_4 alvikite phase, crystallized at the close of crystallization of the carbonate groundmass after the formation of the Fe-Ti oxide reaction rims that removed Fe and Ti from the magma.

ACKNOWLEDGMENTS

We want to express our gratitude to Norman F. Williams, Director of the Arkansas Geologic Commission, for the generous financial support the Arkansas Geologic Commission furnished for instrument and time charges for the microprobe analyses. The Graduate College of the University of Iowa kindly furnished partial subsidy for drafting and photographic charges. J. V. Smith, as always, was most helpful in furnishing us with microprobe standards and allowing us time on the Chicago microprobe. Samples from Perryville, Oppelo dump, and Brazil Branch were supplied by K. C. Jackson of the University of Arkansas, Fayetteville. The figures were ably drafted by Mark Morton. We are indebted for the time and effort of an unknown reviewer whose critical and accurate review forced a rethinking of the data that has resulted in this revised draft.

REFERENCES

- Bence, A.E., and Albee, A.L. (1968) Empirical correction factors for the electron microanalysis of silicates and oxides. *Journal of Geology*, 76, 383–403.
- Croneis, C.G., and Billings, M.P. (1930) Igneous rocks in central Arkansas. *Arkansas Geological Survey Bulletin*, 3, 437 p.
- Erickson, R.L., and Blade, L.V. (1963) Geochemistry and petrology of the alkali igneous complex at Magnet Cove and Potash Sulfur Springs, Arkansas. U.S. Geological Survey Professional Paper 425, 95 p.
- Gaspar, J.C., and Wyllie, P.J. (1982) Barium phlogopite from the Jacupiranga carbonatite, Brazil. *American Mineralogist*, 67, 997–1000.
- Heinrich, E.W. (1980) The geology of carbonatites. Robert E. Krieger Pub. Co., Huntington, New York.
- Leake, Bernard A. (1978) Nomenclature of amphiboles. *American Mineralogist*, 63, 1023–1052.
- Le Bas, M.J. (1977) Carbonatite-nephelinite volcanism. Wiley, New York.
- Kapustin, Y.L. (1980) Mineralogy of carbonatites. Amerind Pub. Co., New Delhi.
- Mitchell, J.R. (1979) The petrology of metamorphic xenoliths in carbonatite intrusions of west-central Arkansas. M.Sc. thesis, University of Arkansas, Fayetteville.
- Reed, S.J.B., and Ware, N.G. (1975) Quantitative electron microprobe analysis of silicates using energy-dispersive X-ray spectrometry. *Journal of Petrology*, 16, 499–519.
- Rimsaite, J. (1969) Evolution of zoned micas and associated silicates in the Oka carbonatite. *Contributions to Mineralogy and Petrology*, 23, 340–360.
- Steele, K.F., and Wagner, G.H. (1979) Relationship of the Murfreesboro kimberlite and other igneous rocks of Arkansas. In F.R. Boyd and H.A.O. Meyer, Eds. *Second International Kimberlite Conference, Proceedings*, vol. I, p. 393–399. American Geophysical Union, Washington, D.C.
- Williams, J.F. (1890) The igneous rocks of Arkansas. *Arkansas Geological Survey Annual Report*, 2, 457 p.
- Wones, D.R., and Eugster, H.P. (1959) Biotites on the join phlogopite ($KMg_3AlSi_3O_{10}(OH)_2$)—annite ($KFe_3AlSi_3O_{10}(OH)_2$). *Carnegie Institution of Washington Annual Report 1958–1959*, 127–132.

MANUSCRIPT RECEIVED NOVEMBER 8, 1985

MANUSCRIPT ACCEPTED SEPTEMBER 2, 1986